The Origin of Outflows in Evolved Stars
Proceedings IAU Symposium No. 366, 2022
L. Decin, A. Zijlstra & C. Gielen, eds.
doi:10.1017/S1743921322001156

Accretion-powered Outflows in AGB Stars

Raghvendra Sahai[1], Jorge Sanz-Forcada[2] and Carmen Sanchez-Contreras[2]

[1]Jet Propulsion Laboratory, Pasadena, CA, USA
email: raghvendra.sahai@jpl.nasa.gov

[2]Centro de Astrobiología (CSIC-INTA), ESAC, Villanueva de la Cañada, Madrid, Spain

Abstract. One of the big challenges for 21st century stellar astrophysics is the impact of binary interactions on stellar evolution. Such interactions are believed to play a key role in the death throes of 1-8 $M_\odot$ stars, as they evolve from the AGB stars into Planetary Nebulae. X-ray surveys of UV-emitting AGB stars show that ∼40% of objects with FUV emission and GALEX FUV/NUV flux ratios $\gtrsim$0.2 have variable X-ray emission characterized by very high temperatures (Tx∼35-160 MK) and luminosities (Lx∼0.002-0.2 $L_\odot$). We hypothesize that such AGB stars have accretion and (accretion-powered) outflows associated with a close binary companion. UV spectroscopy with HST/STIS of our brightest object (Y Gem) shows the presence of infalling and outflowing gas, providing direct kinematic confirmation of this hypothesis. However, the UV-emitting AGB star population is dominated by objects with little or no FUV emission, and we do not know whether the UV emission from these is intrinsic to the AGB star or extrinsic (i.e., due to binarity). Here we present the first results from a large grid of simple chromospheric models to help discriminate between the intrinsic and extrinsic mechanisms of UV emission for AGB stars.

Keywords. (stars:) circumstellar matter, (stars:) binaries (including multiple): close, stars: evolution, stars: AGB and post-AGB

1. Introduction

Most stars in the Universe that leave the main sequence in less than a Hubble time (i.e., stars in the 1–8 $M_\odot$ range) undergo extraordinary deaths, expelling half or more of their masses at rates up to $\sim 10^{-4} M_\odot$ yr^{-1}, as they evolve from the Asymptotic Giant Branch (AGB), through the pre-Planetary Nebula (PPN) to the Planetary Nebula (PN) evolutionary phase. Almost all of our current understanding of this late evolutionary stage of these stars is based on single-star models. However, imaging surveys of (i) the mass-ejecta in PPNe and PNe that show dramatic departures from spherical symmetry (elliptical, bipolar and multipolar morphologies) (e.g., Sahai & Trauger 1998; Sahai et al. 2006, 2007; Sahai, Morris & Villar 2011), and of (ii) AGB circumstellar envelopes that reveal spiral patterns (Decin et al. 2020) have made it increasingly clear that strong binary interactions play a major role in the deaths of low and intermediate-mass stars.

Unfortunately, observational evidence for close binary companions in AGB stars has been generally scarce because AGB stars are very luminous and variable, invalidating standard techniques for binary detection (e.g., radial-velocity and photometric variations due to a companion star, and direct imaging.) However, UV photometric observations can be used to search for binarity and associated accretion activity in AGB stars because most of these are relatively cool ($T_{eff} \lesssim 3000$K) objects (spectral types ∼M6 or later), whereas any stellar companions and/or accretion disks around them are likely significantly hotter

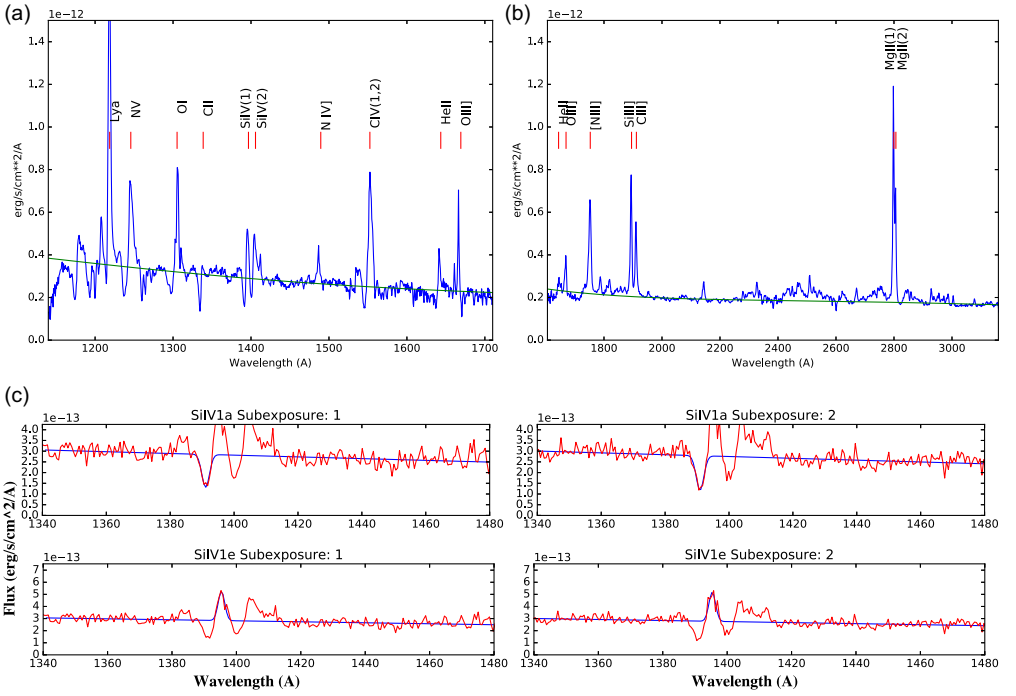

Figure 1. (a,b) Representative HST/STIS spectra of Y Gem, together with a model fit (green curve) consisting of two blackbody components, characterised by $T_{\rm eff}$= 35, 500 K, $L = 6.3\,L_{\odot}$, and $T_{\rm eff}$= 9, 400 K, $L = 6.7\,L_{\odot}$. (c) STIS/UV spectra of Y Gem in the vicinity of the Si IV(1) line for the first two 20 s subexposures. The blue curves show gaussian line-profile fits (together with a linear baseline) to the absorption (top) and emission (bottom) features (*adapted from Sahai et al. (2018)*).

($T_{eff} \gtrsim 6000$K). Hence, favorable secondary-to-primary flux contrast ratios ($\gtrsim$10) are reached in the GALEX FUV ($1344 - 1786$ Å) and NUV ($1771 - 2831$ Å) bands for a source (companion or disk) with $T_{eff} \gtrsim 6000$ K and luminosity $L \gtrsim 1 L_{\odot}$. The feasibility of this technique has been demonstrated in a number of recent studies (Sahai et al. 2008; Sahai, Morris & Villar 2011). From an application of this technique to a volume-limited sample (<0.5 kpc) of 58 AGB stars, Ortiz & Guerrero (2016) conclude that the detection of FUV emission, or an observed-to-predicted ratio for NUV emission of $Q_{NUV} > 20$, are criteria for binarity.

UV spectroscopy can provide an unambiguous probe of accretion-related activity because the latter is expected to produce UV lines with large widths and large Doppler shifts. An HST/STIS spectroscopic study of the prototype fuvAGB star, Y Gem, shows the presence of UV emission lines (Fig. 1) with red (blue)–shifted emssion and absorption features implying high-velocity infall and outflows, as well as short-time-scale variations (flickering). These data directly support the binary/accretion hypothesis (Sahai et al. 2018). The UV spectrum of Y Gem shows lines from species such as Si IV and C IV, with broad emission and absorption features (FWHM$\sim 300 - 700\,{\rm km\,s^{-1}}$) that are respectively, red- and blue- shifted by velocities of $\sim$500 km s^{-1} from the systemic velocity. The UV continuum reveals strong flickering on time-scales of $\lesssim$ 20 s, characteristic of an active accretion disk.

X-ray searches in selected samples of UV-emitting AGB stars, intentionally biased to have relatively high values of the GALEX FUV/NUV ratio ($R_{fuv/nuv}$), as well as serendipitous detections in an archival survey (Ortiz & Guerrero 2021) have also provided

https://doi.org/10.1017/S1743921322001156 Published online by Cambridge University Press

strong supporting evidence for accretion activity in these objects. The X-ray emission is variable, both on long (months–year) and short ($\lesssim few \times 100\,$s)) time-scales. APEC model fits to sources with the highest S/N X-ray spectra show that the observed X-ray luminosity (Lx) and temperature (Tx) lie in the range Lx$\sim (0.002 - 0.2)\,L_{\odot}$ and Tx$\sim (3.5 - 16) \times 10^7\,$K. Dividing the sample of UV-emitting AGB stars into two broad sets, one with high values of $R_{fuv/nuv}(\gtrsim 0.15$, hereafter fuvAGB stars), and one with low values of $R_{fuv/nuv}$ ($\lesssim 0.06$, hereafter nuvAGB stars), we find that X-ray emission is generally detected in fuvAGB stars with $R \gtrsim 0.2$ (including 2 ROSAT detections reported by Ramstedt et al. (2012)). The fraction of X-ray emitting objects for the $R_{fuv/nuv} > 0.17$ sample is 0.4. For stars not detected in X-rays, we find $R_{fuv/nuv} < 0.12$ (with 2 exceptions).

The primary AGB star is very unlikely to be the source of the X-ray emission, since it would require rather strong magnetic fields to confine the hot plasma, and sensitive searches for X-rays in two AGB stars with strong magnetic fields have been unsuccessful (Kastner and Soker 2004) – but the presence of strong local fields confining clumpy hot plasma that can produce the X-ray emission cannot be ruled out. Furthermore, in a recent study, Montez et al. (2017) argue that the origin of the GALEX-detected UV emission is most likely due to a combination of photospheric and chromospheric emission from the AGB star. Their argument is based on finding that for a sample of 179 AGB stars, the NUV emission is correlated with the optical to near-infrared emission. In this study, we investigate whether simple models of chromosphere around AGB stars can reproduce the UV-emission properties of UV-emitting AGB stars.

2. Results

We searched for UV detections by GALEX in a statistical sample of ∼3500 AGB stars with spectral types M4. Our sample was compiled from the Simbad database. A total of 316 objects were detected: $> 20\%$ in one or both of the GALEX FUV and NUV bands, and about $> 9\%$ in both. These percentages are lower limits because most of the GALEX data comes from the All-Sky Imaging Survey (AIS), which had relatively short exposure times, $\sim (1 - few) \times 100\,$s.

2.1. *Red Leak in the GALEX bands*

The filters used to obtain UV photometry are often affected by a "red leak" issue – the leakage of red light through these filters. Generally these leaks are relatively low and do not significantly contaminate the UV flux determinations. According to GALEX documentation, there is no measurable red leak in either the FUV or NUV bands. However for very red stars, such as AGB stars, for which the bulk of the energy is emitted in the red-infrared wavelength region, even a small leak can contaminate the UV flux measurements. We can constrain the "red leak" very sensitively using our sample of AGB stars. We determine the ratios of the FUV and NUV fluxes to the V-band, R-band fluxes, and I-band fluxes, for our sample (and red supergiant stars). The lowest of these ratios can then be considered an upper limit to the red-leak.

The maximum possible red leak for the GALEX FUV and NUV as a fraction of the V-band flux, R-band flux, and I-band flux for AGB O-rich sources and M-type red supergiants stars. We find that the FUV-to-optical band flux ratios are 1.3×10^{-7}, 1.2×10^{-8}, and 1.2×10^{-8} (1.9×10^{-6}, 1.1×10^{-6}, and 3.7×10^{-7}) for AGB stars (red supergiant stars) in the V, R, and I-bands. The NUV-to-optical band flux ratios are 4.0×10^{-7}, 5.8×10^{-8}, and 8.5×10^{-8} (1.5×10^{-5}, 2.7×10^{-7}, and 9.1×10^{-7}) for AGB stars (red supergiant stars) in the V, R, and I-bands. AGB stars thus provide the lowest values of

https://doi.org/10.1017/S1743921322001156 Published online by Cambridge University Press

Table 1. FUV and NUV Variability.

Class	FUV Var			NUV Var			FUV/NUV		
	Ave	Min	Max	Ave	Min	Max	Ave	Min	Max
AGB O-Rich	44%	0.96%	383%	50%	0.05%	306%	0.19	0.003	2.36
Symbiotic	61%	0.8%	214%	61%	0.2%	535%	2.02	0.37	6.93
M supergiants	23%	5.6%	44%	22%	1.4%	120%	0.051	0.021	0.088

the red-leak for both the FUV and NUV bands. The red leak is very low, and does not affect the results of our study.

We compare the UV properties of these 316 AGB stars with two related classes of objects, one in which accretion activity in a binary is known to be important (symbiotic stars) and M-type supergiants, that are believed to possess chromospheres. The sample of supergiants was extracted from the catalog by Hohle et al. (2010). The sample of the symbiotic stars was gathered from the catalog of symbiotic stars by Belczyński et al. (2000). GALEX FUV and NUV data were then extracted for these samples of the supergiants and symbiotic stars as for our AGB stars sample.

2.2. *Comparing the UV Properties of AGB Stars with Other Stellar Classes*

The typical, minimum and maximum values of the variability in the FUV and NUV fluxes, and FUV/NUV flux ratios of these three classes are given in Table 1. The symbiotic sources have the highest average FUV and NUV flux variability (61%), as well as the largest average FUV/NUV ratios. The AGB O-rich sources have FUV and NUV flux variability similar to the symbiotic sources, but their average FUV/NUV flux ratio is about an order of magnitude smaller: ~ 0.19 (O-rich AGB stars) compared to ~ 2 (symbiotic stars). The similarity of the FUV and NUV variability between the symbiotic sources and the AGB O-rich sources reinforcse the idea that the FUV and NUV variability is related to accretion related activity from a binary companion. For our sample of M-type red supergiant stars, which, as a class, are known to possess chromospheres, the average FUV/NUV ratio is signficantly lower, 0.051.

2.3. *Chromospheric Emission*

The mean FUV (f_{FUV}) and the mean NUV (f_{NUV}) for all UV-emitting AGB stars in our sample which were detected in both these bands shows a linear relationship. We find $f_{FUV} = R_{FUV/NUV} * f_{NUV}$ provides a good fit to the bulk of the data, with $R_{FUV/NUV} = 0.061 \pm 0.0015$. Outliers, defined as data where the observed f_{FUV} value was $\geqslant 5\sigma$ away from the model fit, were removed iteratively until the slope and number of outliers converged (in 6 iterations), resulting in the removal of 17 outliers. Restricting our dataset to objects where the SNR for both the mean FUV and NUV was $\geqslant 5$ (a total of 184 objects: Fig. 2(*left*)) did not affect the results significantly – we found $R_{FUV/NUV} = 0.060 \pm 0.0022$ after 5 iterations, with 14 outliers (preliminary results were presented in Sahai et al. 2020).

Previous observations of NUV emission from AGB stars with the IUE, including the presence of strong MgII emission lines, suggested the presence of chromospheres in these stars. Detailed modeling of the NUV IUE spectra, for an M6 AGB star by Luttermoser et al. (1994), shows that a hot chromosphere surrounding the cool photosphere, with temperatures that rise to about $10,000$ K at the outer edge of the former.

We have made a large grid of simple chromospheric models ($\sim 50,000$) using the CLOUDY code (Ferland et al. 2017) and computed the UV emission from a collisionally

https://doi.org/10.1017/S1743921322001156 Published online by Cambridge University Press

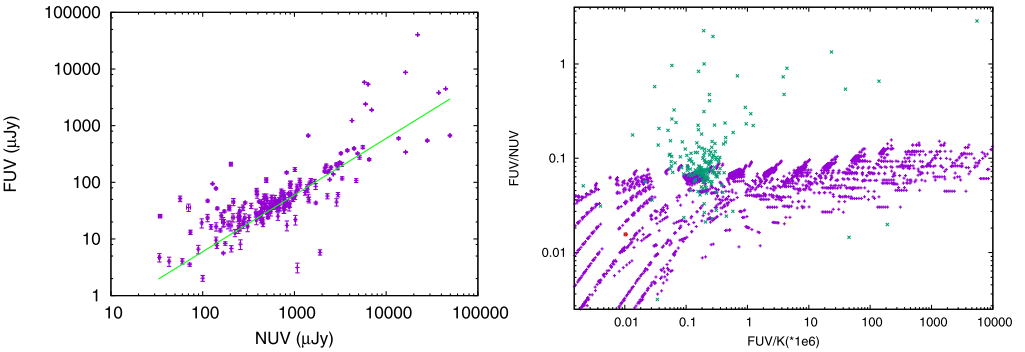

Figure 2. (*left*) The mean FUV– and NUV– band fluxes of AGB stars observed with GALEX, for sources that were detected in both UV bands with a signal-to-noise ratio, SNR$\geqslant 5$. The green line shows a linear least-squares fit with outlier rejection, $f_{FUV} = R_{FUV/NUV} * f_{NUV}$, with $R_{FUV/NUV} = 0.06 \pm 0.002$. (*right*) The observed (green symbols) and model FUV/NUV flux ratio (purple symbols), $R_{FUV/NUV}$, versus the FUV/K-band (2MASS) flux ratio for AGB stars that were detected in both UV bands with SNR of $\geqslant 5$.

ionized plasma with temperature T_{chrom} and density nH contained within a layer of gas of thickness $\Delta\, R$ surrounding the AGB star. These models are characterized by two parameters that describe the AGB star (effective temperature T_{AGB}, and luminosity L_{AGB}), and three parameters that describe the chromosphere (the gas temperature T_{chrom}, the gas density nH_{chrom}, and the thickness of the layer of hot gas, $\Delta\, R$). The range covered by our model grid is as follows: $2500 < T_{AGB}\,(K) < 3300$, $3500 < L_{AGB}\,(L_{\odot}) < 15000$, $3000 < T_{chrom}\,(K) < 16000$, $10.0 < log(nH\,(cm^{-3})) < 16.0$, and $0.0 < log(\Delta\, R\,(cm)) < 7.0$. We adopt a nominal distance of 250 pc and a stellar radius of 10^{13} cm – these parameters do not affect our analysis.

We compute the model FUV and NUV-band fluxes by convolving the model spectra with the GALEX FUV and NUV passbands. We show the observed $R_{fuv/nuv}$ versus the FUV-to-K band flux ratio for our sample of UV-emitting AGB stars, $R_{FUV/K}$, together with model values, in Fig. 2 (*right*) – the latter is a good proxy for the fractional FUV luminosity, since the K-band flux is expected to result almost entirely due to the emission from the AGB photosphere, excluding the effect of the presence of dust that may be present in a stellar wind.

We find that our chromosphere models can produce $R_{fuv/nuv} \sim 0.06$ for temperatures in the range $9,000 \leqslant T_{chrom}\,(K) \leqslant 11,000$. Higher values of $R_{fuv/nuv}$ require higher temperatures, e.g., for $R_{fuv/nuv} \sim 0.1$, we require $11,000 \leqslant T_{chrom}\,(K) \leqslant 15,000$. The allowed values of the parameters $nH\,(cm^{-3})$ and $\Delta\, R\,(\mathrm{cm})$ are not independent; we find $29.5 \geqslant 2 * log(nH) + log(\Delta\, R) \leqslant 31$. This is because the total emission from a collisionally-excited plasma (as assumed for the CLOUDY models) is expected to be proportional to the square of the density, and the total volume of emitting material – the latter is proportional to the thickness since the chromospheric layer is geometrically thin.

We compare our model results to the detailed chromospheric models by Luttermoser et al. (1994), based on fitting near-UV lines from IUE data of the M6 star, g Her, with the greatest weight given to Mg II h and k doublet (~ 2800 Å), followed by Mg I ($\lambda\, 2852$ Å) and the CII] UV0.01 multiplet ($\sim$2325 Å). The temperature distribution of their best-fit model, T10, ranges from 11,270 K to 3,200 K (Fig. 3). The model chromosheric layer extends from the photosphere to a height of ~ 1.7 AU, with temperatures in the range $\sim 9,000 - 11,270$ K at heights $\gtrsim 0.45$ AU. Our simple models thus appear to

https://doi.org/10.1017/S1743921322001156 Published online by Cambridge University Press

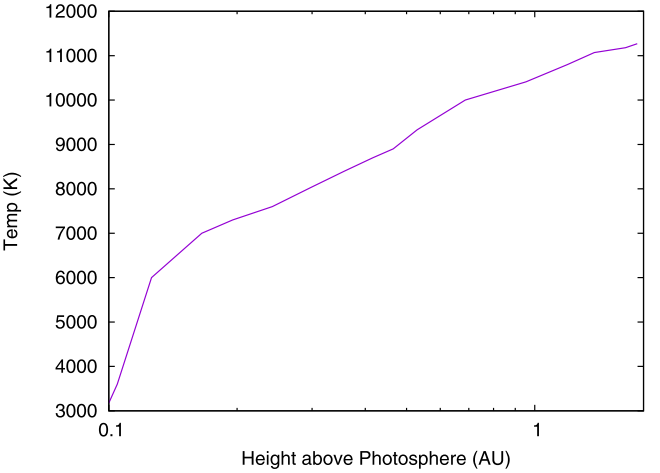

Figure 3. Temperature (T_{chrom}) vs. height above the photosphere for g Her (M6 III) from the best-fit (to NUV lines) chromosphere model of this object (*adapted from Luttermoser et al. (1994)*).

be a reasonable approximation to a more detailed model of the chromosphere for the purpose of investigating the dependence of $R_{fuv/nuv}$ on T_{chrom}.

3. Summary

High-energy observations, at UV and X-ray wavelengths, have provided a new and unique probe into binarity and binary interactions in AGB stars in recent years. The development of models that can fit these data is sorely needed, especially to distinguish between different mechanisms such as accretion-related activity and chromospheric emission. Our simple modeling of hot plasma in AGB stars detected with GALEX in the FUV and NUV bands shows that relatively low values of the FUV-to-NUV flux ratio ($\lesssim 0.06$) may be explained by gas at typical chromospheric temperatures ($\sim 10,000$ K). However, stars with higher FUV/NUV flux ratios require significantly hotter gas, presumably resulting from infall onto an accretion disk around a companion, as confirmed by UV spectroscopic observations of the most prominent UV-emitting star.

Acknowledgements

R.S.'s contribution to the research described here was carried out at the Jet Propulsion Laboratory, California Institute of Technology, under a contract with NASA, and funded in part by NASA via ADAP awards, and multiple HST GO awards from the Space Telescope Science Institute. CSC's work is supported through I+D+i project PID2019-105203GB-C22 funded by the Spanish MCIN/ AEI/10.13039/501100011033. JS-F's work is supported through I+D+i project PID2019-109522GB-C51 funded by the Spanish MCIN/ AEI/10.13039/501100011033.

References

Belczyński, K., Mikołajewska, J., Munari, U., Ivison, R. J., Friedjung, M. 2000. *A&AS* 146, 407–435.

Decin, L. and 34 colleagues 2020. *Science* 369, 1497–1500.

Ferland, G. J. and 10 colleagues 2017. *Rev. Mexicana AyA* 53, 385–438.

Hohle, M. M., Neuhäuser, R., Schutz, B. F. 2010. *AN* 331, 349.

Kastner, J. H., Soker, N. 2004. *ApJ* 608, 978-982.

https://doi.org/10.1017/S1743921322001156 Published online by Cambridge University Press

Luttermoser, D. G., Johnson, H. R., Eaton, J. 1994. *ApJ* 422, 351.
Montez, R., Ramstedt, S., Kastner, J. H., Vlemmings, W., Sanchez, E. 2017. *ApJ* 841, 33.
Ortiz, R., Guerrero, M. A. 2016. *MNRAS* 461, 3036–3046.
Ortiz, R., Guerrero, M. A. 2021. *ApJ* 912, 93.
Sahai, R. & Trauger, J. T. 1998. *AJ* 116, 1357–1366.
Sahai, R., Morris, M., Sánchez Contreras, C., Claussen, M. 2006. in: M.J. Barlow & R.H. Mendéz (eds.), *Planetary Nebulae in our Galaxy and Beyond*, Proc. IAU Symposium No. 234, 499–500.
Sahai, R., Morris, M., Sánchez Contreras, C., Claussen, M. 2007. *AJ* 134, 2200–2225.
Sahai, R., Findeisen, K., Gil de Paz, A., Sánchez Contreras, C. 2008. *ApJ* 689, 1274–1278.
Sahai, R., Morris, M. R. & Villar, G. G. 2011. *AJ* 141, 134–164.
Sahai, R., Sánchez Contreras, C., Mangan, A. S., Sanz-Forcada, J., Muthumariappan, C., Claussen, M. J. 2018. *ApJ* 860, 105.
Sahai, R., Young, O., Sanchez Contreras, C., Sanz-Forcada, J. 2020. *AAS Meeting Abstracts* #235.

https://doi.org/10.1017/S1743921322001156 Published online by Cambridge University Press